Thermal enhanced oil recovery in deep heavy oil carbonates: Experimental and numerical study on a hot water injection performance

Aysylu Askarova [a,*], Aman Turakhanov [a], Strahinja Markovic [a], Evgeny Popov [a], Kirill Maksakov [b], Gennady Usachev [b], Valery Karpov [c], Alexey Cheremisin [a]

[a] *Integrated Center for Hydrocarbon Recovery, Skolkovo Institute of Science and Technology, Moscow, Russia*
[b] *Lukoil LLC, Moscow, Russia*
[c] *Ritek LLC, Moscow, Russia*

ARTICLE INFO

ABSTRACT

Currently, thermal methods of enhanced oil recovery are based on the use of heat transfer mediums (steam, hot water) and *in-situ* combustion, which are the most efficient methods in the development of heavy oil reservoirs. In this study, experimental and numerical modeling was carried out to estimate the efficiency of hot water injection to engage in the active development of high-viscosity oil reserves in a deep carbonate reservoir. There is a limited amount of published experimental studies on carbonates, in comparison with sandstones, shale, or oil sands. Oil-bearing formations at depths of 1100–1500 m require technology that can achieve sufficiently high fluid temperature (250–300 °C) in the bottom-hole zone to be successful. The performance of the implemented technique on a field greatly depends on the quality of the experimental data and numerical simulation. Particularly, the hydrodynamic model, reaction kinetics, and operational parameters are crucial parameters for future upscaling.

The hot water injection experiment was conducted using a medium pressure combustion tube assembly on the reservoir rock model made of consolidated carbonate samples. Moreover, a new numerical model was constructed to simulate the experiment with a reproduction of the fluid models, properties of the oil and rock samples, and full geometry of the core holders where chemical interactions occur. What makes this model authentic is the calibration of reaction kinetics called "aquathermolysis" to hot water injection process, which replicate the most prevalent thermal process during the interaction of hot water and hydrocarbons.

A close correlation between experimental and numerical results was obtained in terms of cumulative water and oil recovery and temperature profiles. The developed numerical model reflects the dynamics of oil displacement at different rates of water injection. According to experimental and numerical simulations, thermal effects reduce viscosity with a proportionate increase in oil recovery. The achieved recovery factor for the experiment was 63%. Lastly, a good match of cumulative gases (CH_4, H_2, H_2S, CO_2, and HMWG) was obtained for the hot water injection experiment. Adapted fluid model, relative permeability, kinetic model, and operational parameters are necessary for the upscaling to the field. The improved efficiency of oil displacement at this site is confirmed by numerical simulation.

1. Introduction

The development of unconventional hydrocarbon resources, including heavy oil fields, can lead to a significant boost of petroleum production worldwide. On average primary and secondary techniques demonstrate recovery factors below 30% for unconventional reservoirs (Bentley, 2002; Pu et al., 2019). Carbonate reservoirs hold more than 60% of the world's oil, and more than 1600 billion barrels of heavy oil (Sola and Rashidi, 2008). Their development requires an application of suitable enhanced oil recovery (EOR) method, selected based on comprehensive studies, including physical and numerical modeling on reliable experimental data and modern software, as well as pilot tests on representative sites of the reservoir. Therefore the primary goal of these studies is to understand reservoir's highly complex distribution of

---

permeability, porosity and flow mechanisms, fluids saturation, as well as geochemistry and associated likelihood of the rock decomposition and carbon dioxide production at high temperatures (Fadaei et al., 2010; Shojaiepour et al., 2014).

These are the reasons why thermal EOR methods are the most widely applied and well-studied techniques (Belgrave et al., 1993; Gutiérrez et al., 2012; Kim and Kovscek, 2017). All of them are based on the heating mechanism while delivered heat decreases oil viscosity within the treated formation (Kapadia et al., 2010, 2009). The classification depends on the mechanism of heat generation in the reservoir. Thermal processes generally can be divided into categories such as hot water injection, steam injection, and in-situ combustion (Pwaga et al., 2010; Terry, 2001).

Nowadays, steam injection is the most widely used and advanced thermal EOR method. Steam is generated on the surface and is pushed down along the injection wells, into the reservoir under high pressure. When steam enters the reservoir, the temperature of the formation significantly increases and the oil viscosity reduces accordingly. That is the main mechanism of heavy oil recovery. Other mechanisms, such as thermal expansion of the oil and capillary forces reduction, also result in additional oil recovery. However, along the reservoir, as the steam cools down and condenses, the lighter hydrocarbons are vaporized or turned into gasses by hot water. With time, the gasses cool down, as they move ahead of the steam and condense back to the oil. The described phenomena give additional gas drive and are called steam stripping (Pwaga et al., 2010; Speight, 2016; Terry, 2001). However, in deep and thin reservoirs steam injection faces difficulties due to overburden heat losses (Rego et al., 2017).

In contrast to steam methods, during *in-situ* combustion, the burning front is generated inside the reservoir, by injecting an oxidizing gas (air or O_2-enriched air). The special heater in the well ignites the oil in the reservoir. The flow of the fire moves, whereas the front moves a mixture of hot combustion gasses, steam, and hot water. It leads to a reduction of oil viscosity and the displacement of oil toward production wells (Bousaid and Ramey, 1968; Gutiérrez et al., 2012; Kisler and Shallcross, 1997; Moore et al., 1996; Moore et al., 2007; Xu et al., 2001; Yang et al., 2017; Yang and Gates, 2009; Yang and Chen, 2016).

In hot water flooding, to decrease the viscosity of heavy oil, a significant amount of hot water is injected into the wells to decrease the viscosity and subsequently displace the oil more easily towards oil production wells (Alajmi et al., 2009; Pwaga et al., 2010). Although hot water injection (HWI) has some drawbacks in comparison with steam EOR, lower transport capacity, heat losses in transport, and displacement efficiency, in the given circumstances, it can be the most attractive alternative. HWI has many attractive points: it can be used in case of the presence of clays in the reservoir, where steam injection cannot be applied; it is also more efficient in maintaining reservoir pressure. (Terry, 2001). Thus, it might be a preferable option in deep reservoirs where high injection pressure is needed and delivery of high-quality steam is not possible. Among several thermal methods, the HWI method is a less expensive process, it requires lower investments and lower levels of heat in comparison with steam injection (Alajmi et al., 2009; Pwaga et al., 2010; Rego et al., 2017; Sola and Rashidi, 2008; Terry, 2001). However, the design of steam and HWI projects requires estimation of casing temperatures and wellbore heat losses, by using methods of determining the overall heat transfer coefficient from the process variables (Stone et al., 2013).

The selected EOR technique must fit the reservoir, its rock and fluid environment (Jha and Verkoczy, 1985) and ensure the feasibility of the project (Dickson et al., 2011). The driving factors affecting the choice of EOR technologies or screening criteria are the depth of the reservoir, porosity, permeability, initial oil saturation, properties of the core, physicochemical properties of oil such as gravity and viscosity, and injectant availability (Surguchev et al., 2010; Taber and Martin, 1983). Depending on these parameters the injection type and EOR method can be chosen for the particular project (Dickson et al., 2011). The

implementation of EOR methods requires high capital investments, it is time and labor-consuming (Taber and Martin, 1983). The prior appropriate planning, which includes technical, and economical screening, modeling and engineering design are essential steps, that can help in the success of the project.

For this research, in-situ combustion was removed from consideration due to the unfavorable quantity of existing wells and their relative positions in field along with, high initial oil saturation and low native oil mobility (Oskouei et al., 2010). On the other hand, the steam injection method was already examined as one of the most promising techniques. However, analytical calculations, trial numerical simulation and wide range of publications (Huygen and Huitt, 1996; Satter, 1965; Stone et al., 2013) indicate that high heat losses might be expected at the targeted depth (1200–1300 m), which corresponds to high pay zone. This method becomes unfeasible at this depth due to the high reservoir pressure (water-steam phase state boundary). Also, steam injection requires expensive casing designs to provide high-quality steam at the bottomhole, as well as ground equipment. Other methods, such as gas and polymer injection were also examined. Detailed description of huff-and-puff CO_2 injection on the same field is presented in paper by (Shilov et al., 2019) where recovery factor was 43%. Polymer flooding was rejected due to reported problems with polymer injectivity and economical concerns (Needham and Doe, 1987; Rego et al., 2017). Due to these factors, it was decided to further proceed with the HWI method.

The HWI method can be applied for carbonate reservoirs at depths of 1200–1300 m as an alternative for steam injection. Due to the limitations of maximum injected temperatures the hot water flooding also can become inefficient due to heat losses (Rego et al., 2017). Successful implementation of HWI requires the selection of optimal conditions for the injection process, especially the temperature and dynamics of injection and production. The heat exchange process leads to changes in the properties of oil after heat exposure and the composition of the extracted produced gases. The nature and rate of these changes strongly influence the feasibility of the selected method. Thus, for the successful realization of the thermal EOR project, the quantification of these processes is of crucial importance. The most reliable way to achieve this is by performing simulations using both physical and numerical models (Kim and Kovscek, 2017) and these models must be obtained before the design of the pilot works. It is necessary to identify all the uncertainties, determine the optimal parameters, and make a prediction of its applicability on the considered field. In this study, we present the experimental results from the HWI treatment of the naturally consolidated carbonate reservoir rock at *in-situ* conditions. Following the in-depth analysis of the experimental results, the numerical simulation was conducted to history-match the HWI process and associated chemical reactions. The results of these analysis laid down a foundation for further development of the upscaled model for the given heavy oil carbonate reservoir. Consequently, the study was performed in two stages – experimental modeling and numerical modeling.

Experimental modeling of the HWI represented a major technical challenge primarily due to the difficulty to safely replicate the high pressure and temperature (P-T) conditions in a deep carbonate reservoir. To begin with, the P-T conditions of the experiment (16 MPa and 270 °C) went well over the P-T rating of the standard core flooding equipment (e. g. Hassler sleeves, sealing gels and heat shrinkable tubes (Feldmann et al., 2020; Kim and Kovscek, 2017)). Fortunately, the combustion tubes (CT) which are primarily used for emulation of the combustion processes and associated chemical reactions, can operate in these conditions. The main downside of CT assemblies is that they require the rock samples to be crushed to improve the combustion reaction (Fadaei et al., 2011). In contrast, for HWI and other flooding methods, performing the experiments on rock samples in their unaltered state is of vital importance. To address this, we developed a technique for injecting a heat-resistant cement, which enabled us to fill the void space between the steel core holder and samples inside it, and therefore ensure the injected water flows through the porous medium, instead of passing it
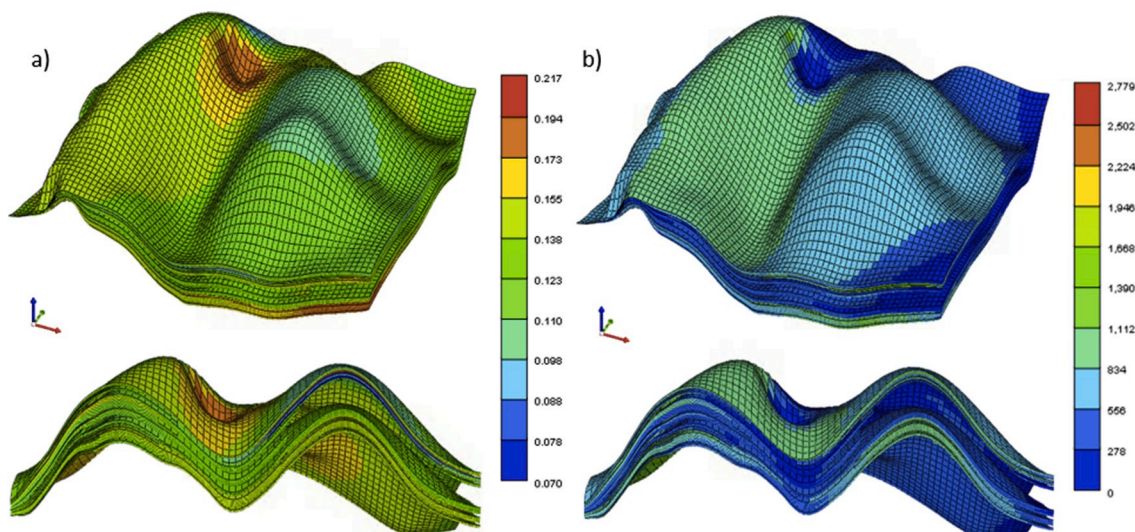
Fig. 1. Porosity (a) and permeability (b) distributions for formation under the study.

by. Additionally, a custom steel core holder with heaters and thermo-couples was manufactured so that a model temperature can be controlled and monitored during the HWI experiment.

The second major challenge of this study was the generation of a proper numerical model. One of the most important aspects of thermal EOR methods is to take into account the extent of chemical transformations from reactants to products. This includes posing questions like "How fast the chemical reactions occur?", and "Which reactions dominate heat exchange process?". These questions cannot be neglected, particularly at temperatures higher than 235 °C (Kapadia et al., 2012). Fortunately, there are several reaction schemes for aquathermolysis published in the literature (Belgrave et al., 1993; Clark et al., 1987; Guangshou et al., 2009; Hyne et al., 1982; Lamoureux-Var and Lorant, 2005; Moore et al., 1996; Tamanyan, 2015) describing different features such as "aquathermolysis window" in the ranges of 170–300 °C; bitumen decomposition where reservoir minerals act as catalysts, etc. (Kapadia et al., 2012). Kinetic models developed for in-situ combustion with pseudo-components can be taken as a basis (Belgrave et al., 1997; Belgrave et al., 1993; Fadaei et al., 2011; Gutiérrez et al., 2012; Kapadia et al., 2012; Lin et al., 1984; Ungerer et al., 1988; Yang and Gates, 2009; Yasar et al., 2001). Aquathermolysis describes chemical reactions occurring during steam or HWI in the presence of certain reservoir minerals such as calcite and dolomite(Fan, 2003; Hyne et al., 1982). Adapted reaction scheme for aquathermolysis of heavy oil proposed in this study can reproduce the cumulative oil, water, and gases produced during the experiment (Kapadia et al., 2012,

2010, 2009). Pseudo-components used in the reaction scheme provide a better understanding of the experimental data. An iterative process of history matching can reproduce the experimental data or history data of the field production. The kinetic model validated by these adjustments is later used to estimate the future performance of the field under research. The adapted fluid model, relative permeability, chemical reaction model, and operational parameters can be used in the sector model for future predictions. According to the results, the thermal EOR method based on HWI can be implemented on the investigated carbonate deep reservoir and a reliable numerical model for further upscaling is obtained. This work is divided into three parts: (1) materials and experimental procedure, (2) development and calibration of the numerical model, (3) and discussion.

2. Materials and experimental procedure

2.1. Cores and oil samples

The reservoir rock samples (core) used for the construction of the physical model were recovered from the heavy oil deep carbonate reservoir in the Russian Federation. The target formation's porosity and permeability were evaluated using standard gas porosity-permeability tests, and they were found to be 17%, and 993 mD on average, respectively. The depth of sample recovery was in the range of 1100 m–1150 m. The spatial distribution of porosity and permeability of the given reservoir is illustrated in Fig. 1.
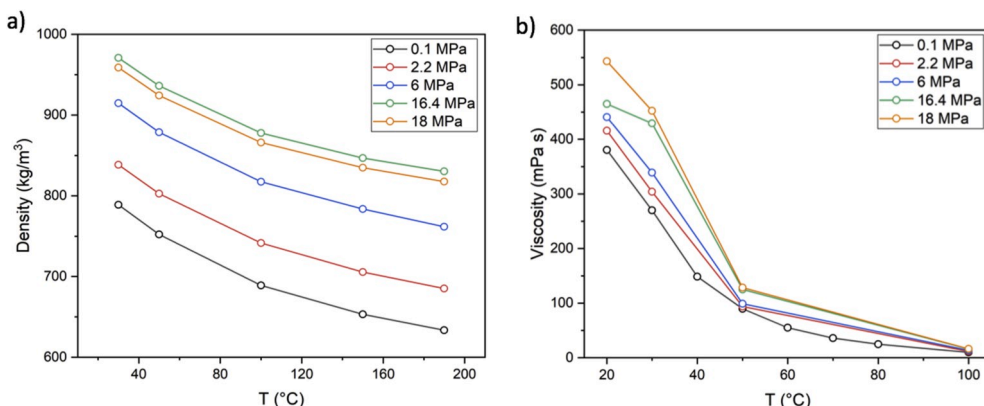

Fig. 2. Temperature dependence of the oil samples density (a) and viscosity (b) at different pressures.
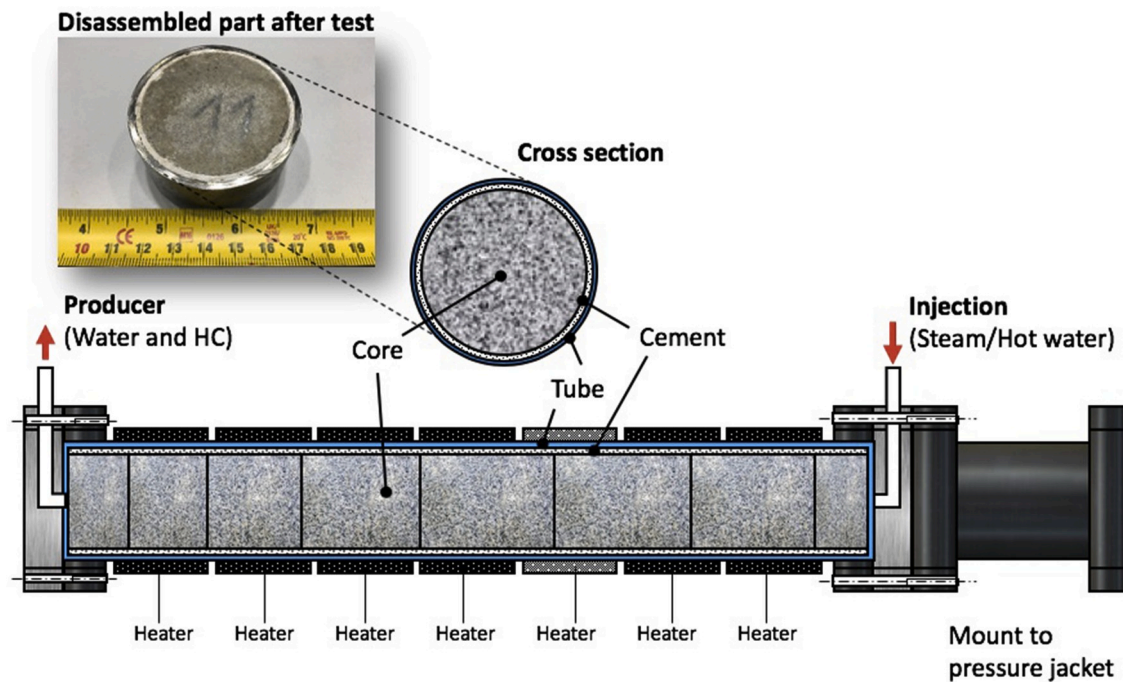
Fig. 3. Scheme of the large core holder for MPCT setup.

In terms of mineralogical composition, the samples were predominantly composed of calcite (67%–100%) with an admixture of dolomite (0%–32.6%). Full-sized core samples were selected for drilling cylindrical core plugs of 49 mm in diameter for the creation of the physical model which would be subjected to the laboratory tests. Samples were taken based on well-log data from sections which were previously identified as pay zone and non-pay zone.

The oil samples were recovered from the same formation. Considering that all oil samples were collected at a wellhead, the oil recombination procedure was required to restore its initial gas content. The samples were further thoroughly homogenized using an overhead stirrer during 48 h. The water content in the samples was determined using Karl Fischer volumetric titration using a Mettler Toledo T5 automatic titrator according to the ASTM E1064-16 standard (<0.5 wt%) (Jílková et al., 2017). The density measurements of oil samples were carried out on a laboratory densitometer DMA 4200 M manufactured by Anton Paar using the cyclic attenuation method. Viscosity measurements of oil were carried out using Anton Paar MCR 302 rotational rheometer equipped with a high-pressure cell. Temperature dependencies of oil sample density and viscosity at different pressures are given in Fig. 2. As expected, a temperature increase has a stronger effect on the viscosity of oils than pressure.

The density and viscosity of oil sample was measured under wide range thermobaric conditions which excluded the need for use of empirical correlations for possible extrapolation. This dataset was subsequently used as an input for CMG WinProp simulator and eventually for the development of the numerical 3D model of MPCT assembly in CMG STARS. This enabled us to perform further simulations for evaluating the applications of HWI.

2.2. Core holder design, cementation and MPCT apparatus

A hot water injection (HWI) experiment was performed on an adapted medium pressure combustion tube (MPCT) assembly (Khakimova et al., 2020; Kudryavtsev and Hascakir, 2014). As mentioned, the custom-made core holder was manufactured out of stainless steel alloy, compositionally similar to the steel grade 304. The wall thickness was 2 mm. Detailed design and model specifications are shown in Fig. 3 and

Table 1
Characteristics of the HWI experiments to determine k_{dis}.

Model specifications	Value
Reactor inner diameter, mm	53
Length, mm	640
Consolidated core diameter, mm	49
Estimated PV of the model, cm^3	203.8
Average model porosity	14.7%

Table 1, respectively.

Fig. 4 (b) shows the core model, composed out of 17 core samples stacked on top of one another. Each sample was 49 mm long in diameter. All samples were cleaned using a soxhlete extractor using toluene at 60 °C, in 2 cycles which were 72 h in total. Following the core model insertion into a vertically mounted core holder, the mixture of high-temperature resistant cement was injected from bottom to top using a proprietary pressure-feed pump as seen in Fig. 4 (a). After the 24 h drying period at ambient conditions (STP), the core holder was placed in an oven at a temperature of 75 °C for another 24 h.

Furthermore, to ensure that the phase flow occurs primarily within the core pore space, it was necessary to confirm that the cement mass did not contain interconnected fractures, that could act as conduits for liquids during the test. The quality of cementation was evaluated using the GE Phoenix L 240 X-Ray CT scanner. The 3D X-ray CT scans of the model were used for visual evaluation of cementation quality in all three planes (XY, XZ, and YZ). Fig. 5 shows that cement mass was uniformly distributed along the core holder, without the presence of elongated fractures or networks of fractures, therefore confirming that the cementation was successful.

Next, the core model was vacuumed for 12 h at −1 bar, and then saturated with reservoir water for 24 h in order to allow the rock-water system to reach the ion exchange equilibrium. Then, water was displaced from the core with recombined live oil at reservoir temperature and pressure maintained by the backpressure regulator until the water fraction in the produced fluid was negligible. After water displacement, oil saturation reached 74%. The confining pressure was 5 MPa higher than reservoir pressure. The parameters of the prepared model are
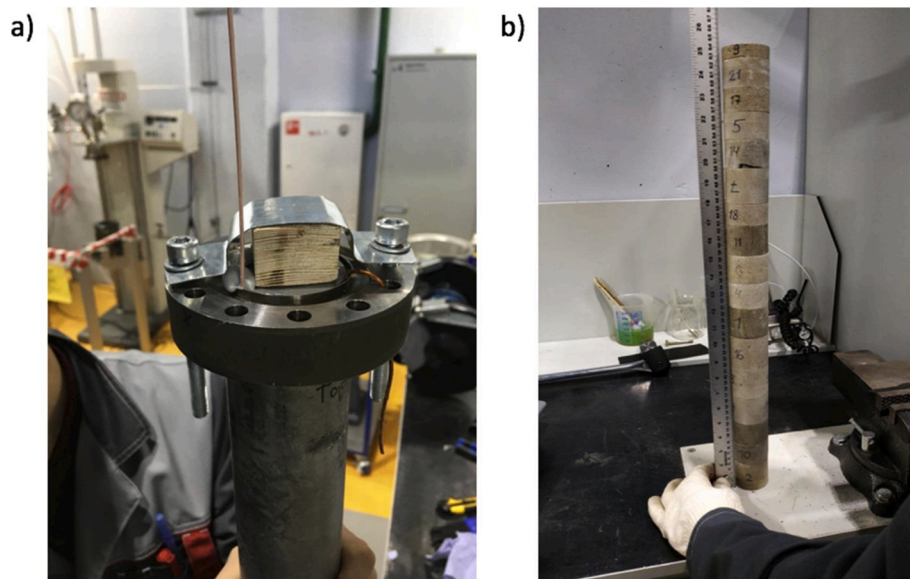
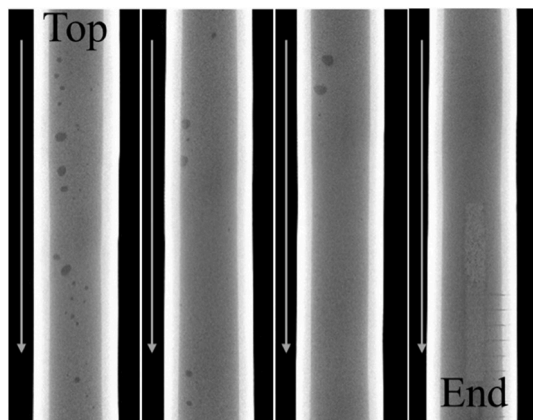**Fig. 4.** Injection of cement into a core holder (a) and a stack of 17 core samples (b).

Fig. 5. Quality of cementing on a computed tomography.

Table 2
Model and reservoir parameters of the experiment.

Parameter	Value
Reservoir pressure, P_{res}, MPa	11
Reservoir temperature, T_{res}, °C	27
Confining pressure, P_{con}, MPa	16
Temperature, °C	250–270
Injection rate S_1, ml/min	1.0
Injection rate S_2, ml/min	2.5
Injection rate S_3, ml/min	5.0

shown in Table 2.

Fig. 6 illustrates the simplified MPCT assembly which was used for the experiment. This type of setup can achieve the temperature up to 1200 °C, and pressure up to 21 MPa.

For temperature control, eight annular heaters and thermocouples were installed on the core holder. During the experiment, fluids displaced from the model were collected in a liquid sampling system. The volume of the produced gases was monitored by a gas meter. Gas sample was taken at regular intervals into the samplers for subsequent analysis by gas chromatography.

3. Development and calibration of numerical model

To conduct a series of numerical experiments, a 3D radial model of the MPCT experiment setup was constructed. The numerical simulation of the experiment was carried out with CMG STARS commercial software using the properties of the recombined oil sample of the studied carbonate oil field. The reliability of the model significantly depends on the quality and integrity of the provided experimental data. Results such as temperature profiles, pressure drops, fluid production dynamics, and operational parameters, are further used in the numerical model of the experiment. The core holder is modeled in a 3D radial coordinate system consisting of five grid blocks in the radial direction, one block in the azimuthal direction, and 26 blocks in the vertical direction (Fig. 7).

As was mentioned earlier, the four central blocks are representing the core, cement, steel wall, and heating blocks. The fifth layer was introduced to represent the upper and lower steel flanges where partial heat losses occur. The importance of the reproduction of multilayer design and simulation of heater regimes is described in the paper (Khakimova et al., 2020). The relative permeability curves were modified to match the cumulative water and oil production. It was determined that the model is highly sensitive to changes in relative permeability.

One of the main steps during the construction of the hydrodynamic model of the proposed oil displacement process is the creation of a representative fluid model. The fluid model was calibrated to reflect the following data obtained from the experiments:

- Physicochemical analysis of oil;
- Density measurements at various values of pressure and temperature;
- Pressure-volume temperature (PVT) experiments;
- Measurements of viscosities at different pressures and temperatures.

The initial pseudo-component composition of the fluid and initial parameters must be specified to determine the state of each pseudo-component (water, maltenes, asphaltenes, N_2, CO_2, O_2) (Tc, Pc, w) based on the physicochemical analysis of oil and data from the standard CMG WinProp library. To create a fluid model in WinGrop CMG format a PVT study of sample from the target field was used. The values are given at reservoir temperature, including the average value of the compressibility coefficient in the range from reservoir pressure to saturation pressure at reservoir temperature. This fluid model further was used in
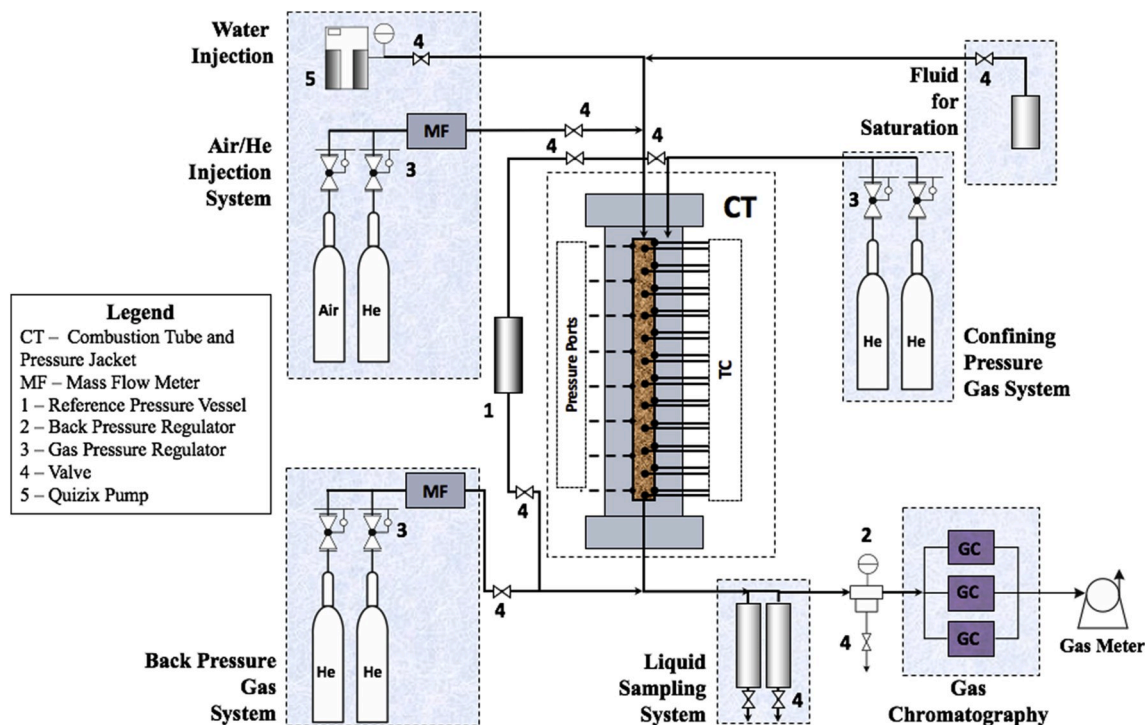
Fig. 6. Schematic diagram of medium pressure combustion tube (MPCT) assembly.
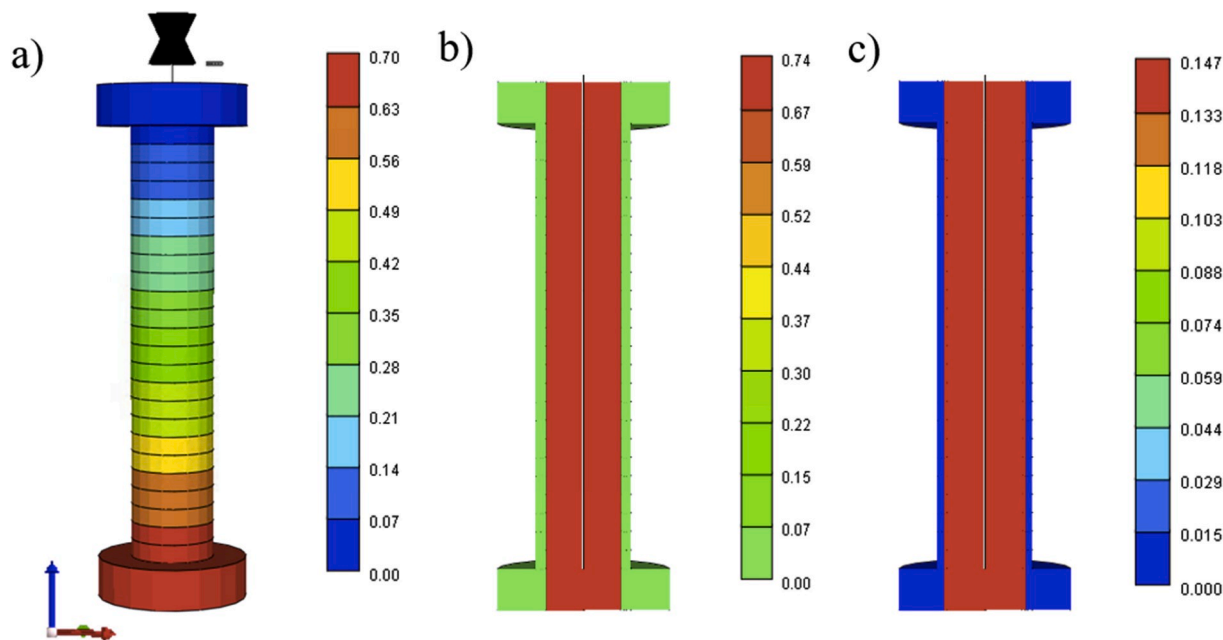

Fig. 7. The numerical model of the CT equipment in CMG: a) grid model; b) porosity; c) initial oil saturation.

the simulations.

The numerical model of MPCT includes a chemical reaction model that is adjusted during the "history matching" process to reproduce the behavior of the given experiment. The main reason to take aquathermolysis reactions into account is hydrogen sulfide, methane, and hydrogen gas presence in the products detected by gas chromatography. Chemical conversion of heavy fractions of oil in the presence of water demonstrated that aquathermolysis reactions could occur through the production of reactive species from organosulfur compounds with their consequent polymerization or reactions with water to produce smaller

fragments such as CH_4, H_2, H_2S, and CO_2 (Hyne et al., 1982; Kapadia et al., 2012).

In the paper by (Kapadia et al., 2012) a detailed description of the aquathermolysis reaction model with associated rate constants was proposed. It was used as an initial model and was "history matched" against the results of the experiment. The heavy fraction of the original oil (C_{8+}) is defined as a pseudo-component "HO" (Heavy Oil); HMWG (High Molecular Weight Gas) is also a pseudo-component that represent combustible hydrocarbon gases (C_{2-7}). HO is in the oleic phase, WATER in aqueous, and other components are in the gas phase. HO as a

Table 3
Pseudo-components and their properties.

Component	Molar Mass, g/mol	Tcrit, °C	P crit, kPa
HO	477	618.85	1418.55
CH_4	16	−82.55	4600.15
H_2S	34	100.05	8937
H_2	2	−240.0	1315
CO_2	44	31.05	7376.46
Water	18	374	22,100
HMWG	58	32.25	4884

Table 4
Kinetic parameters of the reactions.

Component	Frequency factor (A) (day^{-1})	Activation Energy (E) (J/gmol)
1	320	8.12e4
2	7	5.6e4
3	48.95	4.2e4
4	115.025	5.5e4
5	1000	1.2e5

Table 5
Initial conditions.

Property	Value
Oil saturation	0.74
Water saturation	0.26
Gas saturation	0.0
Mole fraction of HMWG (in live oil)	0.0526
Mole fraction of HO	0.9427

pseudo-component can be converted into different products and parallel reactions take place as described in (Kapadia et al., 2012). Carbon monoxide and WATER further react forming carbon dioxide and hydrogen through water gas shift reactions. However, carbon monoxide was not detected by gas chromatography, thus the mentioned reaction was omitted. Adapted ("History matched") reaction scheme is presented below and a list of components with their properties are given in Table 3. Kinetic parameters of the reactions are taken from the experimental data and "history matched" according to the results of the experiment (Table 4). It should be noted, that the activation energy (E_a) values were directly transferred from the (Kapadia et al., 2012), however, frequency factors (A) were adjusted.

1) $1.0 \ HO \rightarrow 236.44 \ H_2$
2) *$1.0 \ HO \rightarrow 29.75 \ CH_4$*
3) $1.0 \ HO \rightarrow 10.84 \ CO_2$
4) $1.0 \ HO \rightarrow 14 \ H_2S$
5) $1.0 \ HO \rightarrow 8.22 \ HMWG$

Table 5 lists the initial physical model conditions at the time when HWI started. The parameters are calculated based on the mass balance data and molecular weight of oil and its fractions.

4. Results and discussion

During the experiment, water preheated to 265–270°C was injected into the model along three stages at different injection rates (Fig. 8). At the first stage, 2.7 PV was pumped through the model, then at the second and third stages, 3.3 and 3.4 PV were injected, respectively. During the first 5 h of the experiment hot water did not heat the whole model due to significant heat losses on massive metal elements of the core holder, that is why the experiment was continued with sequential heating of the entire model to a temperature of 260–270 °C using annular heaters.

Chromatography results of produced gases showed that a large amount of hydrocarbon gases was obtained during the first 5 h of the experiment due to the degassing of recombined oil (Fig. 9). Further temperature increase resulted in the overlapping effect of hydrocarbons distillation and aquathermolysis reactions. When the temperature of the system reached 250–260 °C hydrogen sulfide, methane and hydrogen gas were detected among gas products, which is the main criterion of aquathermolysis reactions taking place. It resulted in a cumulative 1.53 g hydrogen sulfide, 0.011 g hydrogen gas, and 0.067 g methane production.

The first stage of the experiment consisted of 1.1 PV and 1.6 PV of HWI into the consolidated core model before and after the sequential heating of the core holder. It resulted in 35% and 17.3% oil recovery increase only at the first stage. Further rise of the injection rate up to 2.5 ml/min led only to an extra 6% growth of total oil recovery. The ultimate HWI rate of 5 ml/min resulted in only a 5% increase in oil recovery. Extra 3.7% of the oil was obtained after pressure drop and rinsing the outgoing line with toluene. Finally, the experimental set up was disassembled. The tube with a consolidated core was cut and extracted with the alcohol-benzene mixture.

Maltene and asphaltene concentration of the produced oil at the first stage of the experiment was 96.5% and 3.5%, however, for initial oil, it was 90.7% and 9.3%, respectively. Further analysis of the oil density and viscosity also showed that produced at the first stage oil was
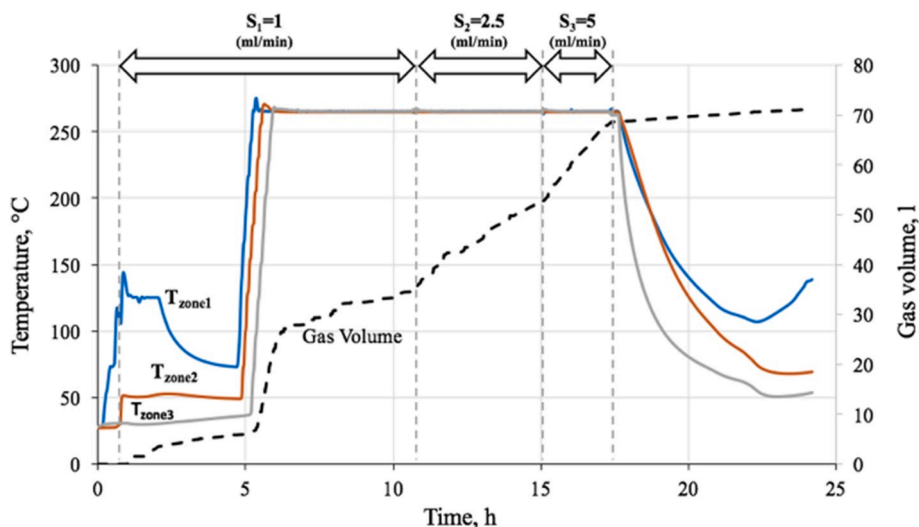

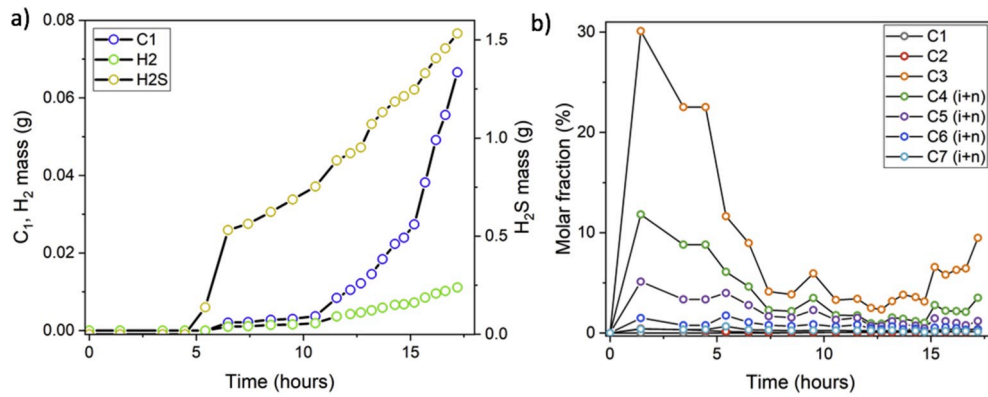**Fig. 8.** Temperatures on the outer wall of the model and cumulative gas volume.

Fig. 9. The molar fraction of produced hydrocarbon gases (aa) and aquathermolysis produced cumulative gas mass (b).

Table 6
Consolidated core model permeability during water saturation and HWI.

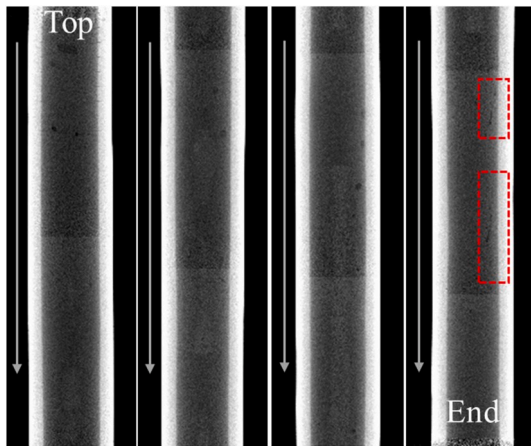| Stage	Viscosity, mPa s	Length, m	Injection rate × 10⁻⁹, m³/s	Pressure drop, MPa	Permeability, mD
Water saturation	1.8	0.644	33.3	0.08	204.1
S_1 = 1 ml/min	0.11	0.644	16.7	0.17	3.06
S_2 = 2.5 ml/min	0.11	0.644	41.7	0.23	5.44
S_3 = 5 ml/min	0.11	0.644	83.3	0.33	7.71

Fig. 10. X-ray scans after the HWI experiment.

upgraded: 131 mPa s and 21.5°API in comparison with 406 mPa s and 19°API, respectively. It also should be noted that the pH values of reservoir water used to saturate the model and produced water differ significantly (6.3 and 8.8, respectively). Thus, we could consider that calcium carbonate decomposition resulted in the ultimate alkalization of

Table 7
Mass of produced oil and water.

Parameter	Experiment	Simulation	Error (fraction)
Mass of produced water, g	1905.0	2126.0	0.116
Mass of produced oil, g	120.0	117.2	0.023

the produced water. However, during the experiment absolute permeability of the consolidated core model increased (Table 6), despite it was about a hundred times less than one estimated during water saturation at ambient conditions.

Analysis of the X-ray CT scans of the core holder after the HWI experiment revealed only minor secondary fractures in the cement mass as shown by red dashed rectangles in Fig. 10. The absence of elongated interconnected indicates that the cementation has successfully provided support and insulation for the samples, thus securing the flow of hot water to occur primarily within the core matrix.

The volume of the oil samples collected during the last two stages was insignificant. It was difficult to separate the emulsion obtained at the last two stages, therefore, determination of the density and viscosity of the oil was canceled.

A comparison of experimental graphs of temperature changes with the corresponding zones of the numerical model is presented in Fig. 11, aa. During the initial period of the first injection stage at the rate of 1 ml/
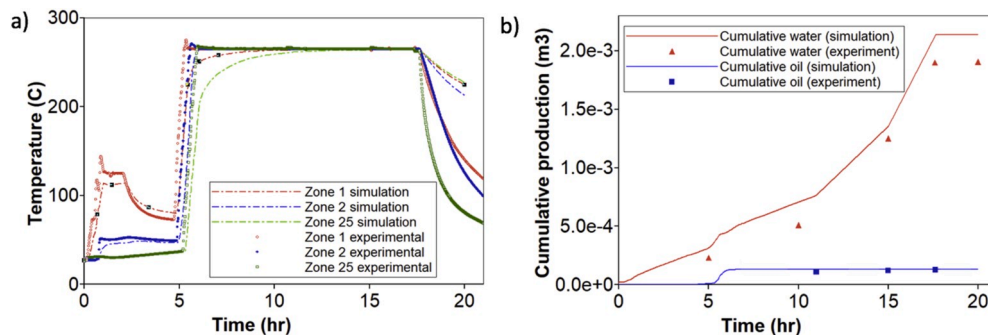

Fig. 11. Temperature profiles (a) and cumulative water and oil (bb) in CMG.
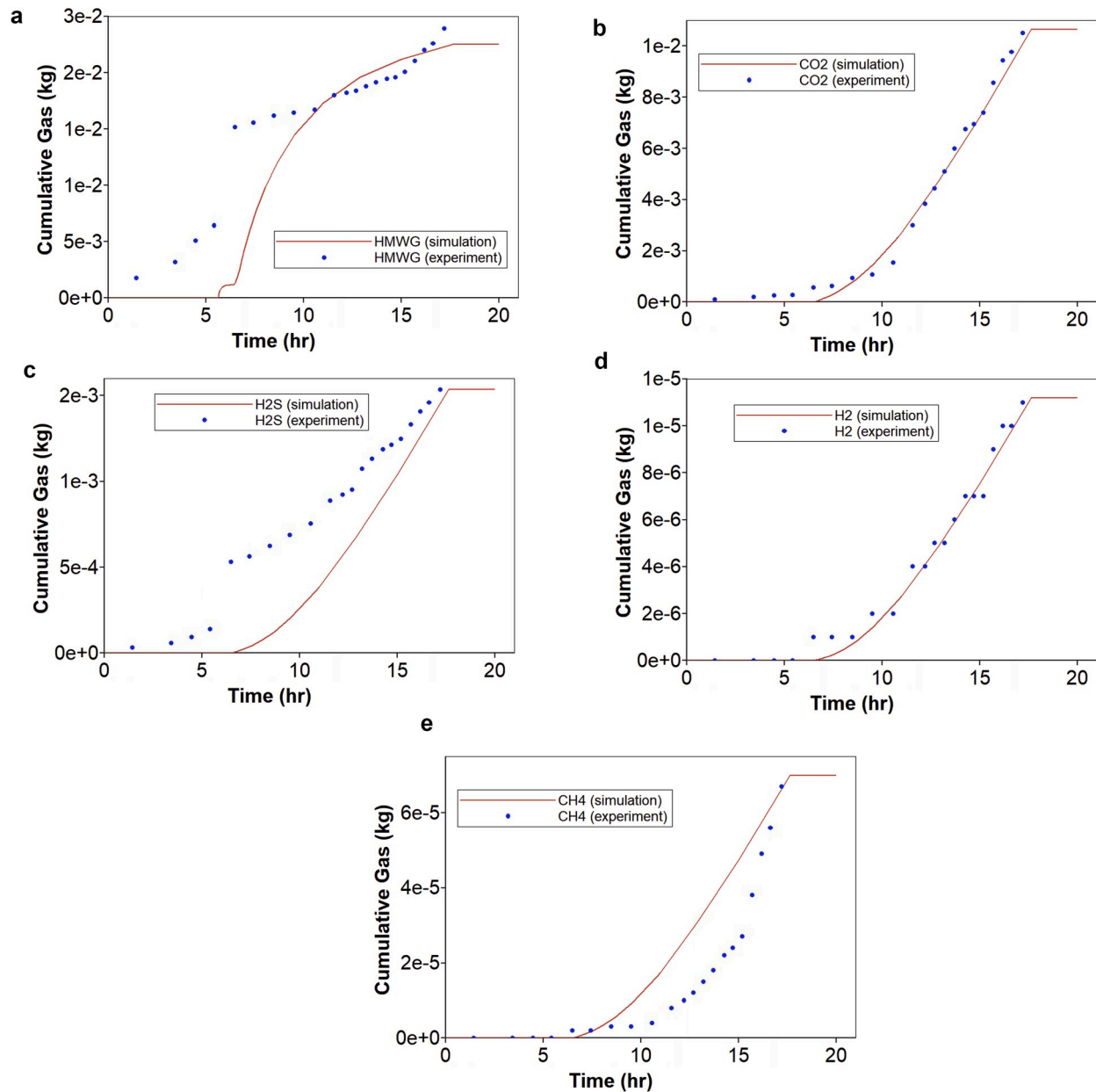
Fig. 12. Cumulative gases.

Table 8
Mass of produced gases.

Parameter	Experiment	Simulation	Error (fraction)
Mass of produced HMWG, g	23.918	22.451	0.061
Mass of produced CO_2, g	10.507	10.332	0.017
Mass of produced H_2S, g	1.533	1.488	0.029
Mass of produced H_2, g	0.110	0.108	0.018
Mass of produced CH_4, g	0.067	0.068	0.015

min, there was no significant increase in temperature on the outer wall due to heat losses. However, even in the initial stage, water was pumped through the model and displaced oil (see Fig. 11, bb).

Table 7 below provides a comparison of the cumulative production of water and oil for the experiment and numerical simulation.

Fig. 12 presents a comparison of the cumulative gas masses for experiment and simulation, while Table 8 gives absolute values of the produced HMWG, CO_2, H_2S, H_2, and CH_4. Results obtained during

simulation demonstrate comparatively good match within 3%, except HMWG which exceeds 6%. It could be explained by the assumption that was made during the simulation. HMWG was initially in the oil phase (recombined oil sample). There are two mechanisms taking place: degassing of original recombined oil (HMWG release) and reaction (5) from Section 3 K-values obtained in WinProp led to numerical problems and significant disagreement in cumulative oil production. Thus, during simulation, it was assumed that gas liberation occurred immediately, and HMWG was initially introduced as a pseudo-component in a gas phase. Table 5 was adjusted accordingly: oil saturation was equal to 69%, and gas saturation was equal to 5%.

It is worth mentioning, that the CO_2 and H_2 curves demonstrate the best match in comparison with H_2S, CH_4, and HMWG. It could be explained due to the variable heating of the model at the first stage of the experiment before switching on the annular heaters. In addition, the sampling of the produced gases was discrete and it might differ from the continuous regime of produced gases. The relative permeability curves introduce additional uncertainty.

The products of the chemical reactions serve as a sign of the presence of aquathermolysis at the studied temperature ranges (200–270°C) or, so-called "aquathermolysis window". Further increase of the temperature (above 300°C) could lead to the thermal cracking reaction and conversion of the heavy molecules into light hydrocarbons and coke (Hyne et al., 1982; Kapadia et al., 2012). The proposed kinetic model takes into account chemical interactions of heavy oil with hot water with consequent formation of acid gases such as carbon dioxide and hydrogen sulfide. H_2S due to its toxicity and environmental concerns has limitations on the percent of its recovery and is an important parameter that should be taken into account. Production of active species from organosulfur compounds and subsequent reaction of the smaller fragments generating CH_4, H_2, H_2S, and CO_2 was also demonstrated.

The results obtained during numerical simulation demonstrate an acceptable agreement of the temperature profiles, cumulative water, oil, and gas values. The model reflects the oil displacement in the first section when water is pumped at the rate of $S_1 = 1$ ml/min, followed by an increase at the transition to the speed of S_2 and S_3. The main part of the oil displacement occurs at the first stage; however, with a further change in the pressure drop, there is a slight yield of oil. Thermal treatment reduces viscosity with a subsequent increase in oil yield.

5. Conclusions

This research provides calibration of the aquathermolysis kinetic model to the HWI process at the temperatures higher than 250 °C. The chemical interactions of heavy oil components with the hot water must be taken into account during process modeling. A common kinetic model of aquathermolysis reactions was adjusted during history matching according to the results of the experiment. The simulation results of the experiment demonstrate a close agreement of temperature profiles, as well as a good match of experimental and simulation values of cumulative fluid output. Gaseous products of aquathermolysis reactions were obtained: hydrogen sulfide, methane, hydrogen gas, carbon dioxide. Cumulative gas masses obtained during numerical simulation demonstrated a very good match with the experimental data. The model correctly reflects the dynamics of oil displacement at different rates of water injection. Evaluation of the history matching quality influences the efficiency of future predictions of the field performance. According to obtained results, the thermal effect of water injection at a temperature of 250–270 °C reduces the viscosity of oil due to heating, increasing its mobility, which leads to high values of recovery factor. The efficiency of oil displacement by HWI for studied oil field is confirmed by numerical simulation.

The robust workflow of experimental and numerical modeling of hot water injection into the heavy oil deep carbonate reservoir was presented. The proposed technology of cementation of consolidated core samples into the core holder for the experiment at temperatures above 250 °C works successfully. The data obtained during the laboratory experiment, as well as during the numerical modeling in a hydrodynamic simulator such as cementation technology, fluid model, relative permeability curves, kinetic model, and operational parameters can be used in the sector model for future predictions. It is the basis for subsequent scaling to a hydrodynamic sector model based on which the optimal rate, optimal injection temperature, and volume of the injectant in the reservoir are selected.

Declaration of competing interest

The authors declare that they have no known competing financial interests or personal relationships that could have appeared to influence the work reported in this paper.

CRediT authorship contribution statement

Aysylu Askarova: Conceptualization, Methodology, Formal analysis, Investigation, Data curation, Writing - original draft, Writing - review & editing, Visualization. **Aman Turakhanov:** Conceptualization, Methodology, Formal analysis, Investigation, Writing - original draft, Writing - review & editing, Visualization. **Strahinja Markovic:** Conceptualization, Methodology, Formal analysis, Writing - original draft, Writing - review & editing. **Evgeny Popov:** Conceptualization, Methodology, Formal analysis, Investigation, Writing - review & editing. **Kirill Maksakov:** Conceptualization, Resources. **Gennady Usachev:** Conceptualization, Resources. **Valery Karpov:** Conceptualization. **Alexey Cheremisin:** Conceptualization, Writing - review & editing, Supervision.

Acknowledgements

Nomenclature

EOR	enhanced oil recovery
HWI	hot water injection
P-T	pressure and temperature
MPCT	medium pressure combustion tube
HO	heavy oil
LO	light oil
HMWG	High Molecular Weight Gas
A	frequency factor
Ea	activation energy
PV	pore volume

Appendix A. Supplementary data

Supplementary data to this article can be found online at https://doi.org/10.1016/j.petrol.2020.107456.

References

Alajmi, A.F., Algharaib, M., Gharbi, R., 2009. Experimental evaluation of heavy oil recovery by hot water injection in a middle eastern reservoir. SPE Middle East Oil Gas Show Conf. MEOS, Proc. 2, 1–14.

Belgrave, J.D.M., Moore, R.G., Ursenbach, M.G., 1997. Comprehensive kinetic models for the aquathermolysis of heavy oils. J. Can. Pet. Technol. 36, 38–44.

Belgrave, J.D.M., Moore, R.G., Ursenbach, M.G., Bennion, D.W., 1993. A comprehensive approach to in-situ combustion modeling. SPE Adv. Technol. 1, 98–107.

Bentley, R.W., 2002. Global oil & gas depletion: an overview. Energy Pol. 30, 189–205. https://doi.org/10.1016/S0301-4215(01)00144-6.

Bousaid, I.S., Ramey, H.J., 1968. Oxidation of crude oil in porous media. Soc. Petrol. Eng. J. 8, 137–148. https://doi.org/10.2118/1937-pa.

Clark, P.D., Dowling, N.I., Lesage, K.L., Hyne, J.B., 1987. Chemistry of organosulphur compound types occurring in heavy oil sands: 5. Reaction of thiophene and tetrahydrothiophene with aqueous Group VIIIB metal species at high temperature. Fuel 66, 1699–1702. https://doi.org/10.1016/0016-2361(87)90366-8.

Dickson, J.L., Leahy-Dios, A., Wylie, P.L., 2011. Development of improved-hydrocarbon-recovery-screening methods. JPT. J. Petrol. Technol. 63, 43–44. https://doi.org/10.2118/0111-0043-jpt.

Fadaei, H., Castanier, L.M., Kamp, A.M., Debenest, G., Quintard, M., Renard, G., 2011. Experimental and numerical analysis of in-situ combustion in a fractured core. SPE J. 16, 358–373. https://doi.org/10.2118/141117-PA.

Fadaei, H., Debenest, G., Kamp, A.M., Quintard, M., Renard, G., 2010. How the In-Situ Combustion Process Works in a Fractured System: 2D Core- and Block-Scale Simulation, pp. 118–130.

Fan, H., 2003. The effects of reservoir minerals on the composition changes of heavy oil during steam stimulation. J. Can. Pet. Technol. 42, 11–14. https://doi.org/10.2118/03-03-N1.

Feldmann, F., Strobel, G.J., Masalmeh, S.K., AlSumaiti, A.M., 2020. An experimental and numerical study of low salinity effects on the oil recovery of carbonate rocks combining spontaneous imbibition, centrifuge method and coreflooding experiments. J. Petrol. Sci. Eng. 190, 107045. https://doi.org/10.1016/j.petrol.2020.107045.

Guangshou, S., Tiyao, Z., Linsong, C., Yunxian, W., 2009. Aquathermolysis of Conventional Heavy Oil with Superheated Steam, pp. 289–293. https://doi.org/10.1007/s12182-009-0046-4.

Gutiérrez, D., Moore, R.G., Ursenbach, M.G., Mehta, S.A., 2012. The ABCs of in-situ-combustion simulations: from laboratory experiments to field scale. J. Can. Petrol. Technol. https://doi.org/10.2118/148754-PA.

Huygen, H.H.A., Huitt, J.L., 1996. Wellbore heat losses and casing temperatures during steam injection. In: Spring Meeting of the Eastern District, API Division of Production, pp. 25–32.

Hyne, J.B., Clark, P.D., Clarke, R.A., Koo, J., Greidanus, J.W., Tyrer, J.D., Verona, D., 1982. Aquathermolysis of heavy oils. Rev. Tec. INTEVEP 2, 87–94.

Jha, B., Verkoczy, K.N., 1985. Oil recovery BY thermal methods. Present. In: 36 Th Annu. Tech. Meet. Pet.

Jílková, L., Hlincík, T., Ciahotný, K., 2017. Determination of water content in pyrolytic tars using coulometric karl-fischer titration. https://doi.org/10.14311/AP.2017.57.0008, 57 8 13.

Kapadia, P.R., Kallos, M.S., Gates, I.D., 2010. A comprehensive kinetic theory to model thermolysis, aquathermolysis, gasification, combustion, and oxidation of athabasca bitumen hydrogen generation from pyrolysis and Aquathermolysis : experimental data. In: Improved Oil Recovery Symposium, pp. 1–31.

Kapadia, P.R., Kallos, M.S., Leskiw, C., Gates, I.D., 2009. Potential for hydrogen generation during in situ combustion of bitumen. In: Society of Petroleum Engineers - EUROPEC/EAGE Conference and Exhibition, vol. 2009, pp. 8–11.

Kapadia, P.R., Wang, J., Kallos, M.S., Gates, I.D., 2012. New thermal-reactive reservoir engineering model predicts hydrogen sulfide generation in Steam Assisted Gravity Drainage. J. Petrol. Sci. Eng. 94–95, 100–111. https://doi.org/10.1016/j.petrol.2012.06.030.

Khakimova, L., Askarova, A., Popov, E., Moore, R.G., Solovyev, A., Simakov, Y., Afanasiev, I., Belgrave, J., Cheremisin, A., 2020. High-pressure air injection laboratory-scale numerical models of oxidation experiments for Kirsanovskoye oil field. J. Petrol. Sci. Eng. 188, 106796. https://doi.org/10.1016/J.PETROL.2019.106796.

Kim, T.W., Kovscek, A., 2017. High-Temperature Imbibition for Enhanced Recovery from Diatomite, pp. 1–21.

Kisler, J.P., Shallcross, D.C., 1997. An improved model for the oxidation processes of light crude oil. Chem. Eng. Res. Des. https://doi.org/10.1205/026387697523859.

Kudryavtsev, P., Hascakir, B., 2014. Towards dynamic control of in-situ Combustion : effect of initial oil and water saturations. In: SPE Western North American and Rocky Mountain Joint Regional Meeting, pp. 1–12.

Lamoureux-Var, V., Lorant, F., 2005. H2S artificial formation as a result of steam injection for EOR: a compositional kinetic approach. In: SPE/PS-CIM/CHOA International Thermal Operations and Heavy Oil Symposium Proceedings, pp. 1–4. https://doi.org/10.2523/97810-ms.

Lin, C.Y., Co Chen, W.H., Co Lee, S.T., Culham, W.E., 1984. Numerical simulation of combustion tube experiments and the associated kinetics of in-situ combustion processes. Soc. Pet. Eng. AIME 657–666. https://doi.org/10.2118/11074-PA.

Moore, R.G., Laureshen, C.J., Ursenbach, M.G., Mehta, S.A., Belgrave, J.D.M., 1996. Combustion/Oxidation behavior of athabasca oil sands bitumen. In: Improved Oil Recovery Symposium. Society of Petroleum Engineers, pp. 1–8. https://doi.org/10.2118/35392-MS.

Moore, R.G., Mehta, S.A., Ursenbach, M.G., 2007. A Guide to High Pressure Air Injection (HPAI) Based Oil Recovery. https://doi.org/10.2118/75207-ms.

Needham, R.B., Doe, P.H., 1987. Polymer Flooding Review. J. Petrol. Technol. 1503–1507. https://doi.org/10.2118/17140-PA.

Oskouei, S.J.P., Maini, B., Moore, R.G., Mehta, S.A., 2010. Experimental evaluation of SAGD-ISC hybrid recovery method. In: Canadian Unconventional Resources & International Petroleum Conference, pp. 1–10. https://doi.org/10.2118/137836-ms.

Pu, W., Zhao, S., Hu, L., Varfolomeev, M.A., Yuan, C., Wang, L., Rodionov, N.O., 2019. Thermal effect caused by low temperature oxidation of heavy crude oil and its in-situ combustion behavior. J. Petrol. Sci. Eng. 184, 1–8. https://doi.org/10.1016/j.petrol.2019.106521.

Pwaga, S., Lluore, C., Hundseth, O., Perales, F.J., Idrees, M.U., 2010. Comparative Study of Different EOR Methods.

Rego, F.B., Botechia, V.E., Schiozer, D.J., 2017. Heavy oil recovery by polymer flooding and hot water injection using numerical simulation. J. Petrol. Sci. Eng. 153, 187–196. https://doi.org/10.1016/j.petrol.2017.03.033.

Satter, A., 1965. Heat losses during flow of steam down a wellbore. In: SPE Production Research Symposium 1966, pp. 845–851. https://doi.org/10.2118/1071-pa.

Shilov, E., Cheremisin, A., Maksakov, K., Kharlanov, S., 2019. Huff-n-puff experimental studies of CO2 with heavy oil. Energies 12, 1–15. https://doi.org/10.3390/en12224308.

Shojaiepour, M., Kharrat, R., Hashemi, A., 2014. Experimental and simulation study of in-situ combustion process in carbonate fractured porous media. J. Japan Pet. Inst. 57, 208–215.

Sola, B.S., Rashidi, F., 2008. Experimental study of hot water injection into low-permeability carbonate rocks. Energy Fuel. 22, 2353–2361. https://doi.org/10.1021/ef800009r.

Speight, G.J., 2016. Oil recovery. In: Speight, J.G. (Ed.), Introduction to Enhanced Recovery Methods for Heavy Oil and Tar Sands, second ed. Gulf Professional Publishing, Boston, p. 493. https://doi.org/10.1016/B978-0-12-849906-1.00019-9.

Stone, T.W., Li, G., Pallister, I., 2013. A comparison of analytic and segmented heat and quality loss in thermal steam injection wells. In: SPE Reservoir Simulation Symposium Held in the Woodlands, pp. 1–11.

Surguchev, L.M., Reich, E.M., Berenblyum, R.A., Schipanov, A.A., 2010. Improved oil recovery methods: applicability screening and potential evaluation. In: Society of Petroleum Engineers - SPE Russian Oil and Gas Technical Conference and Exhibition, vol. 2010, pp. 2–7. https://doi.org/10.2118/134742-ms.

Taber, J.J., Martin, F.D., 1983. Technical screening guides for the enhanced recovery of oil. In: Proc. - SPE Annu. Tech. Conf. Exhib. 1983-Octob. https://doi.org/10.2523/12069-ms.

Tamanyan, B.P., 2015. Aquathermolysis of crude oils and natural bitumen : chemistry , catalysts and prospects for industrial implementation. Russ. Chem. Rev. 84, 1145–1175. https://doi.org/10.1070/RCR4500.

Terry, R.E., 2001. Enhanced oil recovery. Encycl. Phys. Sci. Technol.

Ungerer, P., Behar, F., Villalba, M., Heum, O.R., Audibert, A., 1988. Kinetic modelling of oil cracking. Org. Geochem. 13, 857–868. https://doi.org/10.1016/0146-6380(88)90238-0.

Xu, H.H., Okazawa, N.E., Moore, R.G., Mehta, S.A., Laureshen, C.J., Ursenbach, M.G., Mallory, D.G., 2001. In Situ upgrading of heavy oil. J. Can. Pet. Technol. 40, 45–53.

Yang, M., Harding, T.G., Chen, Z., 2017. An improved kinetics model for in situ combustion of pre-steamed oil sands. Energy Fuel. 31, 3546–3556. https://doi.org/10.1021/acs.energyfuels.6b02582.

Yang, X., Gates, I.D., 2009. Combustion kinetics of Athabasca bitumen from 1D combustion tube experiments. Nat. Resour. Res. 18, 193–211. https://doi.org/10.1007/s11053-009-9095-z.

Yang, M., Chen, Z., 2016. An improved reaction kinetics model of in-situ combustion for pre-steamed oil sands. In: SPE Canada Heavy Oil Technical Conference, pp. 1–16.

Yasar, M., Trauth, D.M., Klein, M.T., 2001. Asphaltene and resid pyrolysis. 2. The effect of reaction environment on pathways and selectivities. Energy Fuel. 15, 504–509. https://doi.org/10.1021/ef0000577.